10.1071/CH16586_AC

Australian Journal of Chemistry 2017, 70(5), 623-631

Supplementary Material

Structure and Magnetic Studies on a Series of Two-Dimensional Iron(II) Framework Materials with Varying Ligand Characteristics

Matthew A. D. Roxburgh,[A] Samantha Zaiter,[A] Xina I. B. Hudson,[A] Benjamin R. Mullaney,[A] John E. Clements,[A] Boujemaa Moubaraki,[B] Keith S. Murray,[B] Suzanne M. Neville,[A,C] and Cameron J. Kepert[A,C]

[A]School of Chemistry, The University of Sydney, Sydney, NSW 2006, Australia.
[B]School of Chemistry, Monash University, Melbourne, Vic. 3800, Australia.

[C]Corresponding authors. Email: suzanne.neville@sydney.edu.au; cameron.kepert@sydney.edu.au

S1. Single crystal structural analysis

*Structure of **pin-S***

A red block-like crystal of **pin-S** was quench cooled to 150(2) K and a full data set collected. The structure was solved and refined using a combination of Direct and Fourier methods.[7,8] Analysis of the systematic absences indicated either *Cc* or *C*2/*c* as possible space groups. Refinement in *C*2/*c* gave a solution with the entire ligand disordered over two sites. Structure solution and refinement in *Cc* gave a model with only disorder in the amide portion of the ligand and hence was assigned as the most appropriate space group. The thermal ellipsoid representation of the asymmetric unit is shown in Figure S1. The disordered atoms in the ligand and the solvent were refined isotropically. All other atoms in the framework were refined anisotropically and hydrogen atoms were attached using the riding model.

There are a series of host–host interactions (N15B···O35B_**7**: 2.90(3), N15A···O15A_**8**: 2.83(2), N15A···O35A_**6**: 2.71(2), N35B···O15B; see figure S3) and host–guest interactions

(C51···O15A_**12**: 3.52(19), C51···O35B: 3.52(18), C61···O35A_**3**: 3.36(18), C61···O5B_**3**: 3.54(20) Å); see figure S4). Operators for generating symmetry equivalents: **3**: x+1/2, -y+1/2, z-1/2, **6**: x+1/2, y+1/2, z, **7**: x, -y+1, z-1/2, **8**: x, -y+1, z+1/2, **12**: x, -y+1, z+1/2.

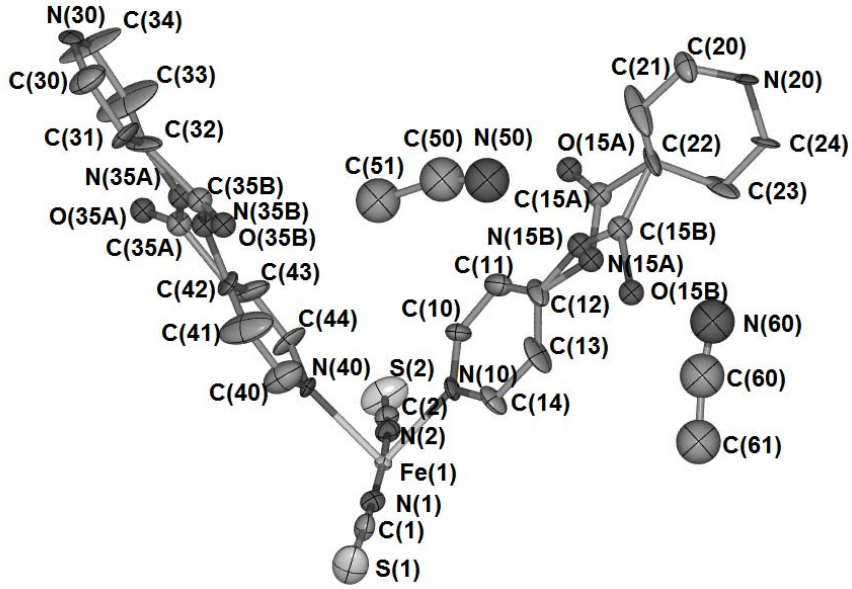

Figure S1. ORTEP representation of the asymmetric unit of **pin-S** (50% ellipsoid probability)**.** Hydrogen atoms have been omitted for clarity.

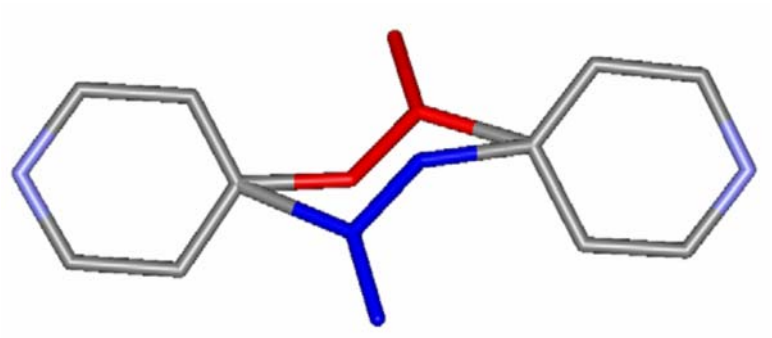

Figure S2. Pin ligand inversion centre disorder observed in both L1 and L2 in **pin-S**.

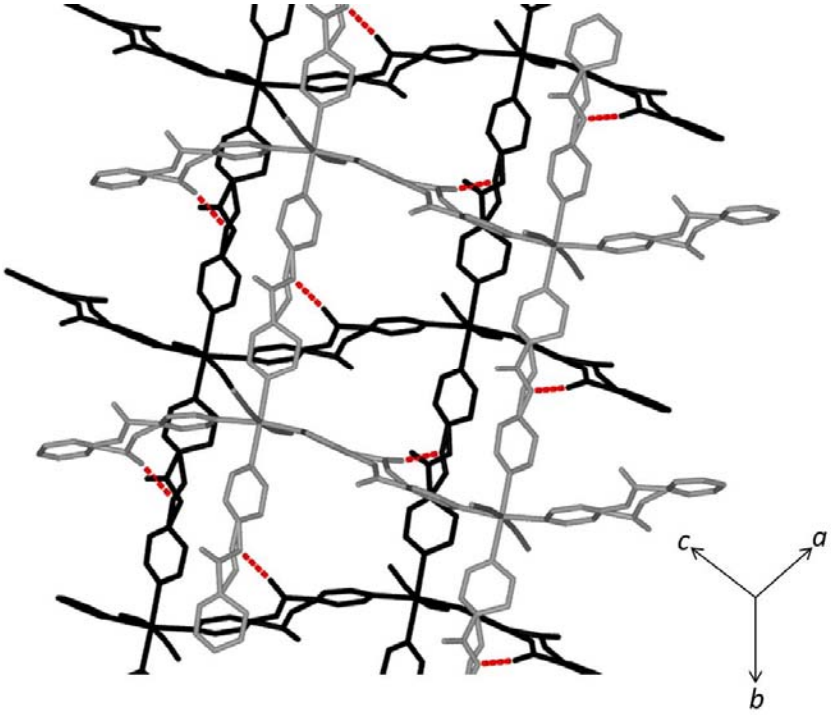

Figure S3. Two adjacent grids of pin-S showing the alternating layer undulation (black and grey) and host–host hydrogen bonding interactions (red).

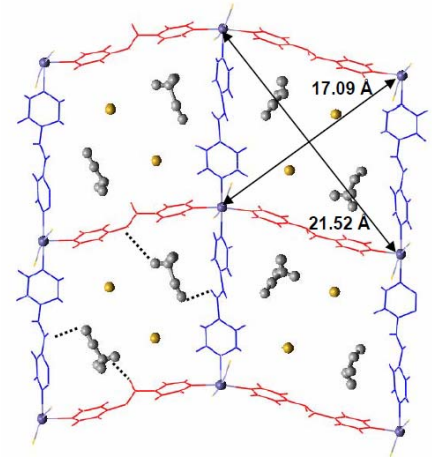

Figure S4. One grid of **pin-S** showing the diagonal Fe···Fe distances and host–guest hydrogen bonding interactions.

*Structure of **tvp-S***

The structure was solved in the triclinic space group $P\bar{1}$. All non-hydrogen framework atoms were modelled anisotropically with hydrogen atoms assigned using geometrical constraints (Figure S5). The disordered ethanol and free tvp guests were modelled isotropically with the displacement parameters of equivalent atoms fixed to be equal and equivalent bond lengths restrained to be approximately uniform within 0.01 esd. The ethanol guest molecule is disordered over two sites and was modelled isotropically constraining equivalent bond lengths and angles to be equal within 0.01 esd. This disorder is illustrated in Figure S6. The occupancy ratios of the two components refined to 73:27. The atomic displacement parameters of equivalent atoms in the disordered ligand were fixed to be equal and the relative occupancy ratios of the two components refined to 55:45.

There are a series of guest–guest interactions between the ethanol solvent molecules in free tvp ligands as depicted in Figure S7 (N70···O80B: 2.833(2) and N60···O80A: 2.836(2) Å).

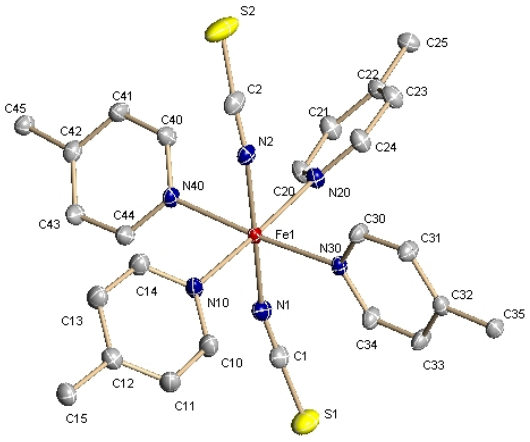

Figure S5. ORTEP representation of the asymmetric unit of **tvp-S** (50% ellipsoid probability)**.** Hydrogen atoms have been omitted for clarity.

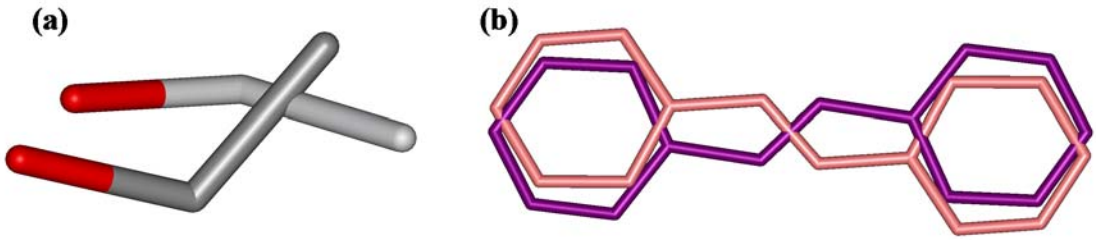

Figure S6. Disorder in (a) the ethanol molecules and (b) the free tvp pyridyl ligand in **tvp-S.**

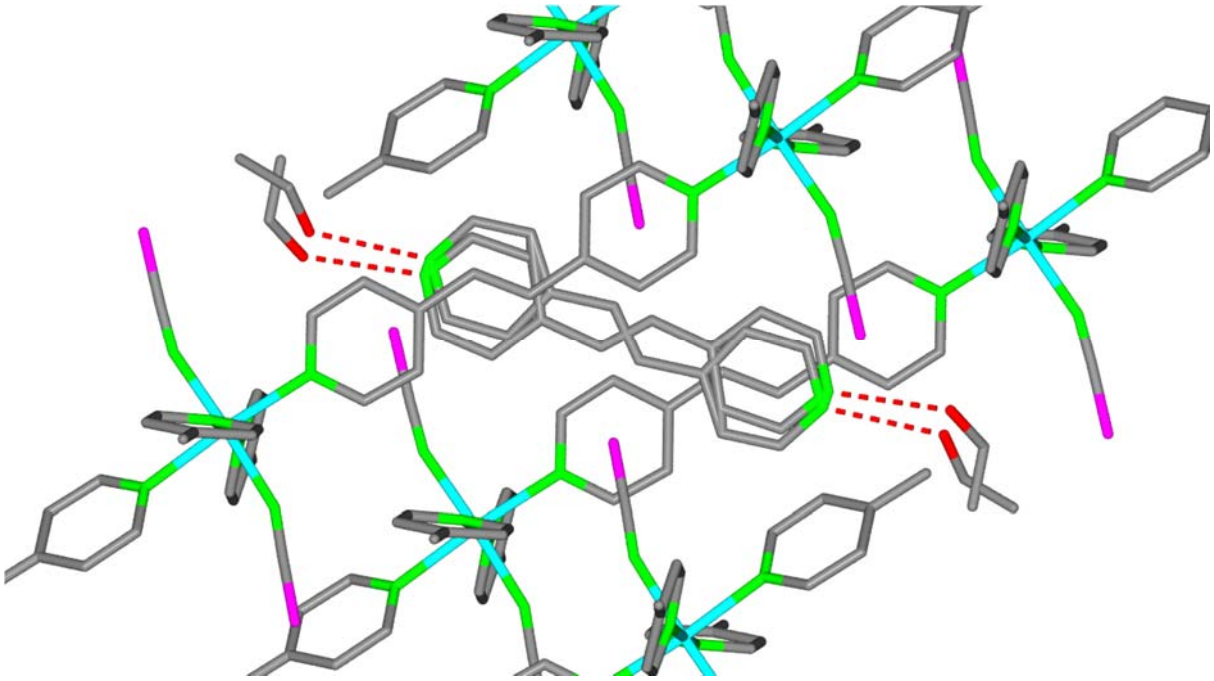

Figure S7. Structural representation of the hydrogen bonding interactions (red) present in **tvp-S** between ethanol molecules and free tvp ligands. Disorder of ethanol and free tvp ligands shown.

*Structure of **dbbpe-S***

All non-hydrogen framework atoms were modelled anisotropically with hydrogen atoms being assigned using geometrical constraints.

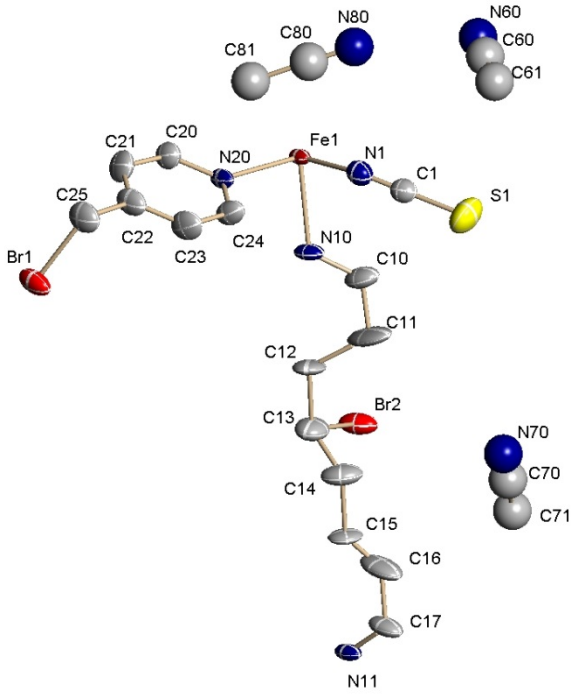

Figure S8. ORTEP representation of the asymmetric unit of **dbbpe-S** (50% ellipsoid probability). Hydrogen atoms have been omitted for clarity.

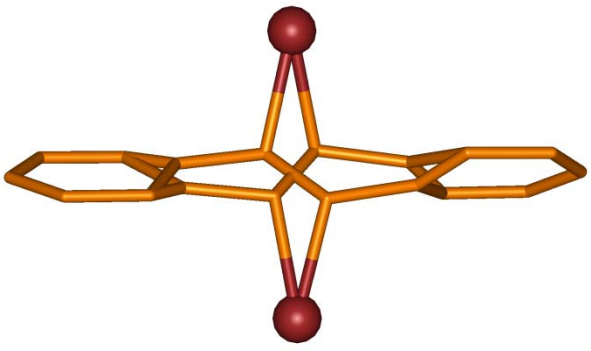

Figure S9. Disorder between the pyridyl rings associated with one of the bridging **dbbpe** ligands.

*Structure of **bptz-S***

All non-hydrogen atoms were modelled anisotropically except for the disordered ethanol molecule, which was modelled isotropically (Figure S10). Hydrogen atoms were placed using the riding model. The number of EtOH molecules present within the structure was determined using the SQUEEZE function in PLATON; the exact solvent loading was difficult to determine as the ethanol molecules occupy a very high proportion (calc. 41%) of the void volume. Only the oxygen atoms of the ethanol molecules were modelled in the structure solution.

The chloroform guests are located within the pore space of each 2-D grid and are involved in hydrogen bonding interactions with the NCS^- anions [(S1···H-C28$(Cl)_3$ = 3.65(2) Å and S2···H-C27$(Cl)_3$ = 3.63(2) Å]. The ethanol molecules are located in the interlayer space, with two of these taking part in hydrogen bonding interactions with the tetrazine ring [(N7···H-O1 = 3.17 (2) Å and N10···H-O7= 3.12(2) Å)]. The stacking is also stabilised by anion–π interactions between NCS^- and the electron deficient tetrazine ring [3.242(14) Å] (Figure S12).

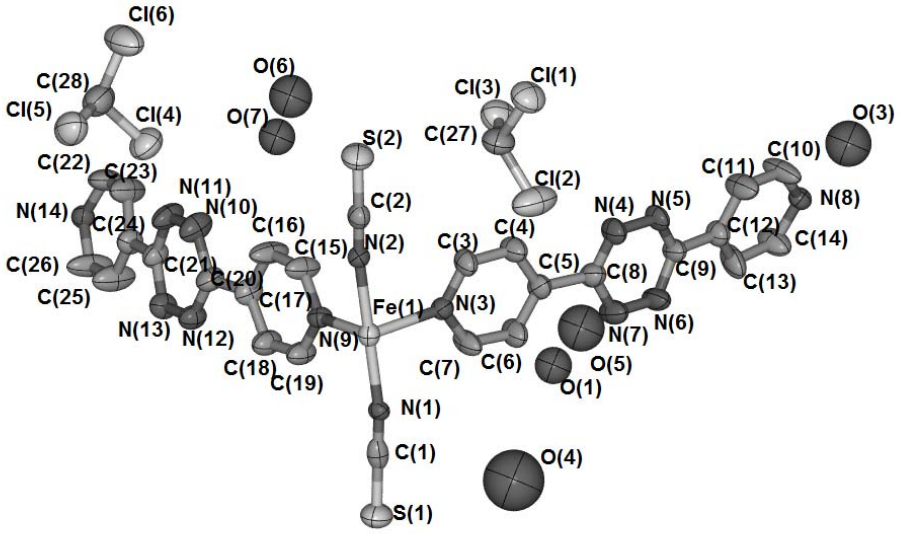

Figure S10. ORTEP representation of the asymmetric unit of **bptz-S** (50% ellipsoid probablity). Hydrogen atoms have been omitted for clarity.

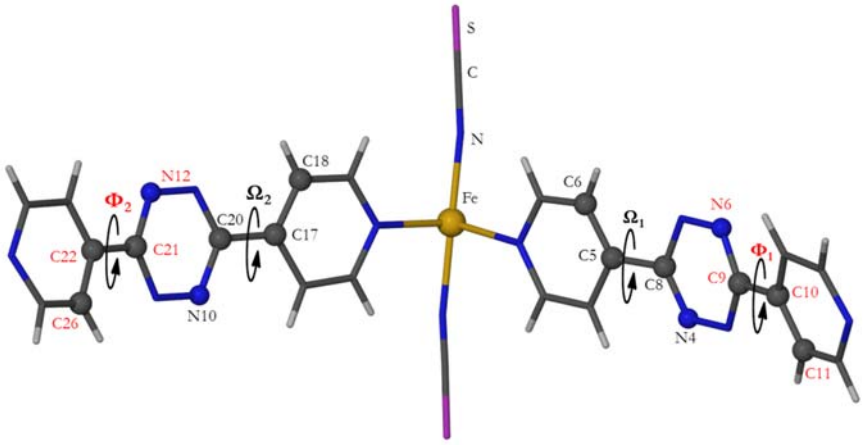

Figure S11. Ball-and-stick representation and **bptz-S** showing the torsion angle between the first pyridyl and central tetrazine ring (Ω) and the last pyridyl and central tetrazine ring (ϕ).

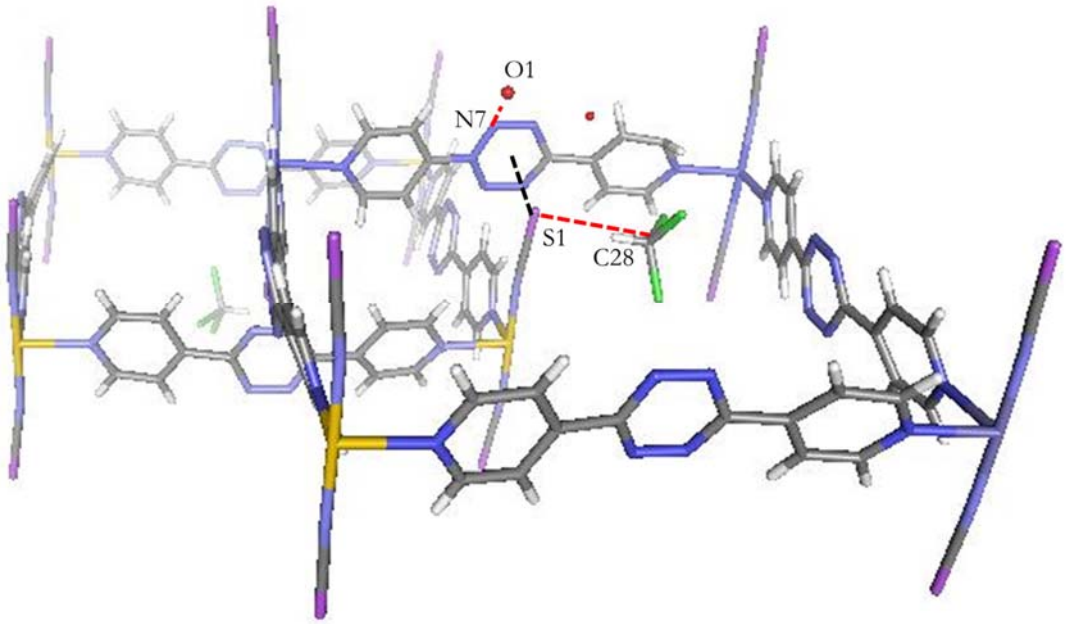

Figure S12. Intermolecular interactions for **bptz-S**.

*Structure of **bptz-Se***

The $NCSe^-$ anions from adjacent layers protrude into the pores and form anion–π interactions [3.31(2) Å] with the electron deficient tetrazine ring of bptz (Figure S15). The $NCSe^-$ anions also form hydrogen bonding interactions with a chloroform [Se1···H-C14 = 3.70(2) Å] and an ethanol molecule [3.18(3) Å] (Figure S15). In contrast to **bptz-S**, all of the solvent molecules are located within the grid pores rather than the interlayer space.

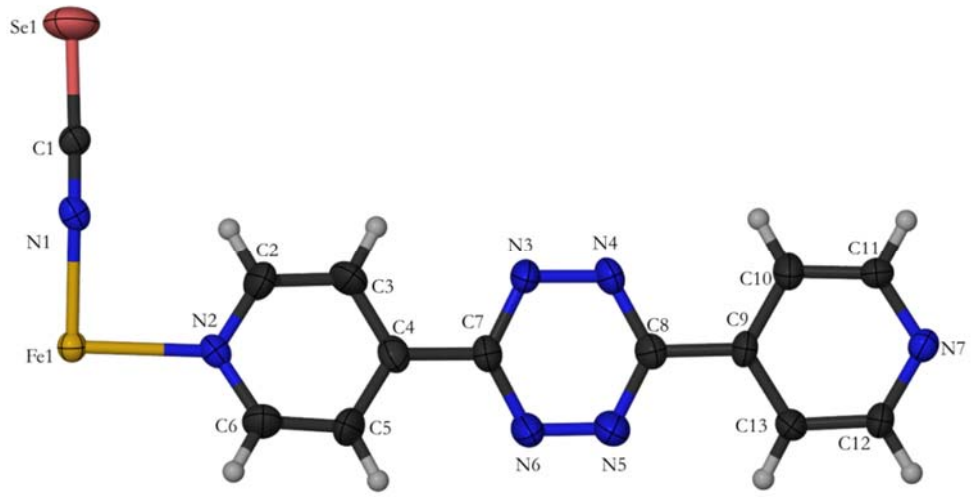

Figure S13. The asymmetric unit of **bptz-Se**. Atoms are shown as 50% thermal ellipsoids and the solvent molecules have been omitted for clarity.

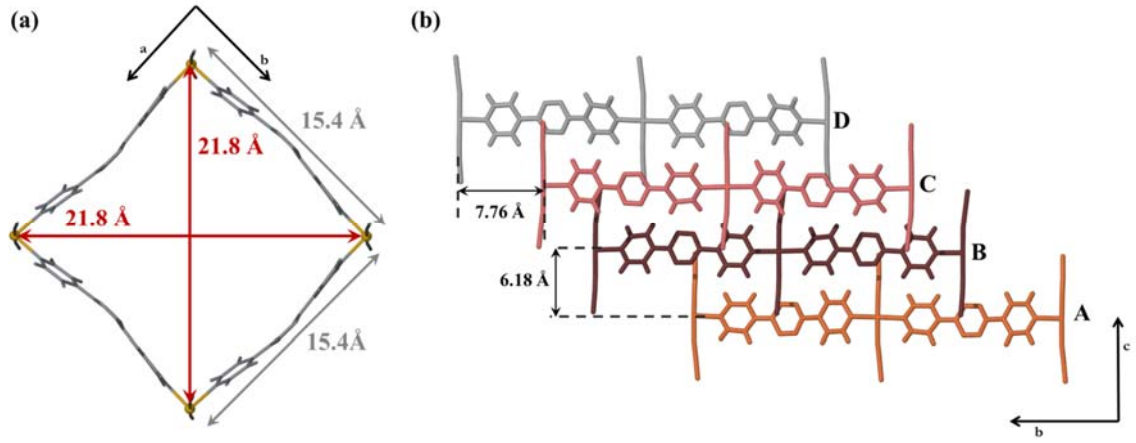

Figure S14. Stick representations of the (a) (4,4) grids and (b) the offset helical stacking of the 2D sheets in **bptz-Se**. Solvent molecules have been omitted for clarity.

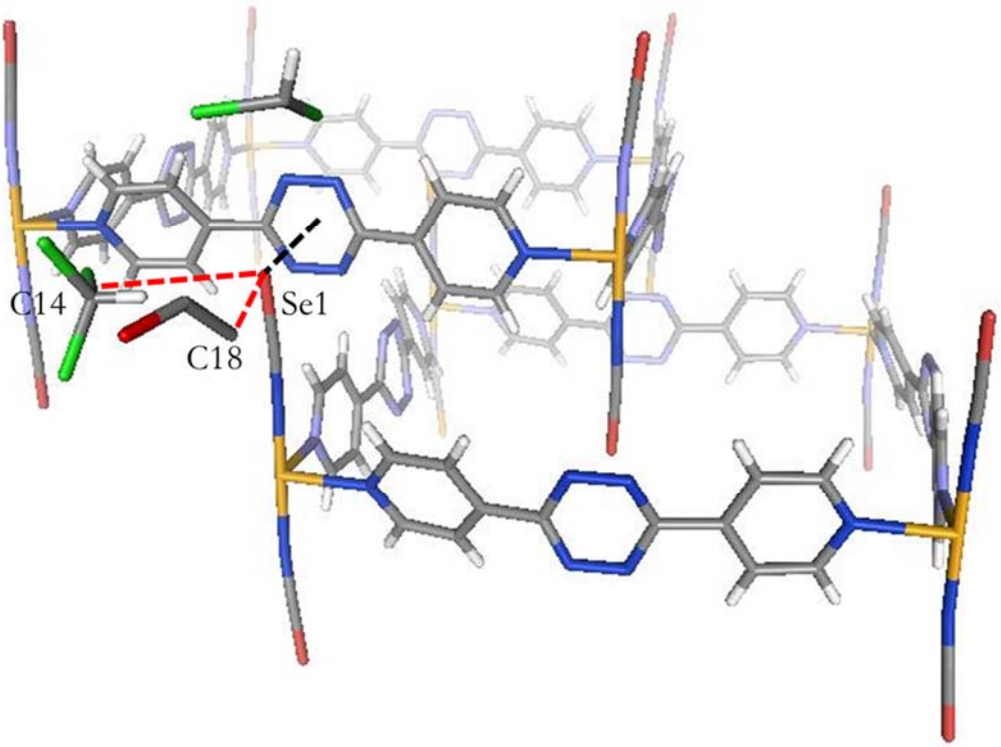

Figure S15. The anion–π interactions (black) between Se1 and bptz and hydrogen bonding interactions (red) between Se1 and solvent molecules in **bptz-Se**.

*Structure of **bpac-S***

All non-hydrogen atoms were modelled anisotropically except for the disordered propanol molecule, which was modelled isotropically (Figure S16). Hydrogen atoms were placed using the riding model.

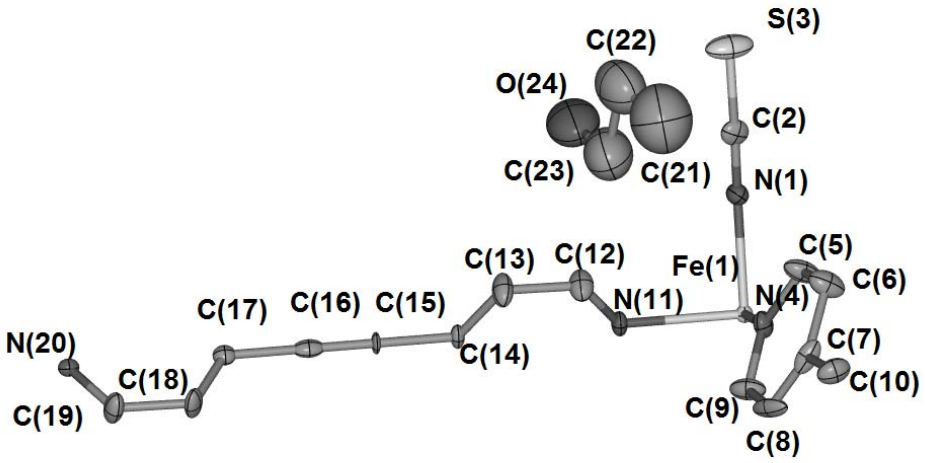

Figure S16. The asymmetric unit of **bpac-S**. Atoms are shown as 50% thermal ellipsoids.

*Structure of **bpeben-S***

All non-hydrogen atoms were modelled anisotropically except for the disordered ethanol molecule, which was modelled isotropically (Figure S17). Hydrogen atoms were placed using the riding model. Owing to the large amount of guest accessible voids filled with disordered solvent the SQUEEZE routine within PLATON was employed.

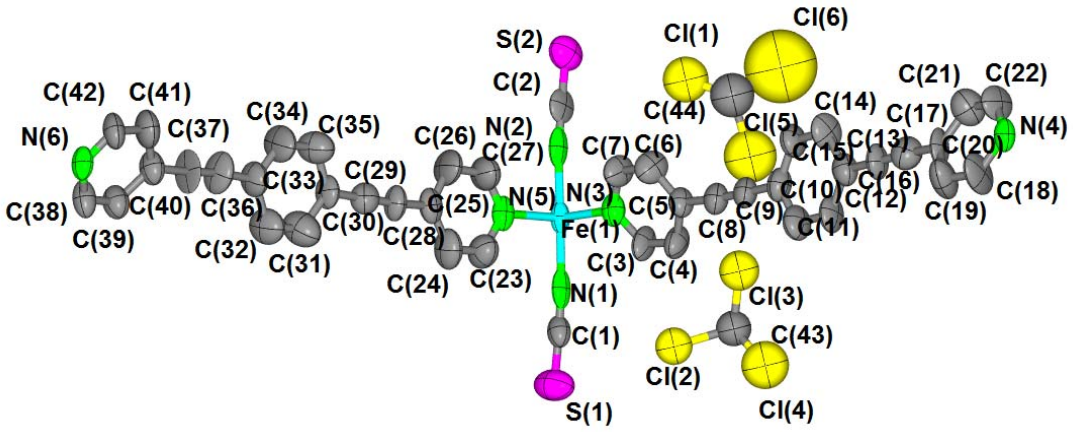

Figure S17. The asymmetric unit of **bpeben-S**. Atoms are shown as 50% thermal ellipsoids, and hydrogen atoms are removed for clarity.

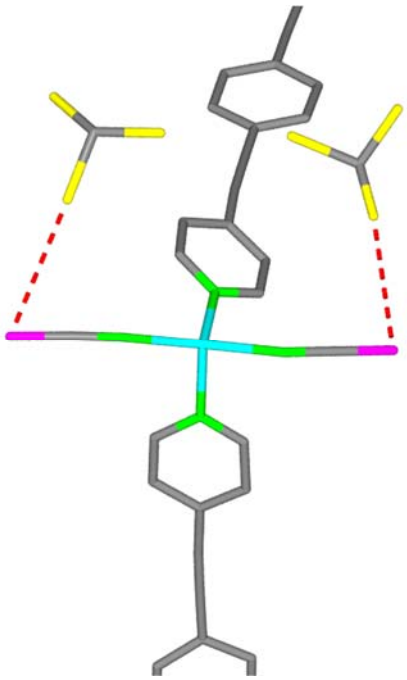

Figure S18. The hydrogen bonding interactions (black) between chloroform and thiocyanate anions in **bpeben-S**.

S2. Magnetic Susceptibility

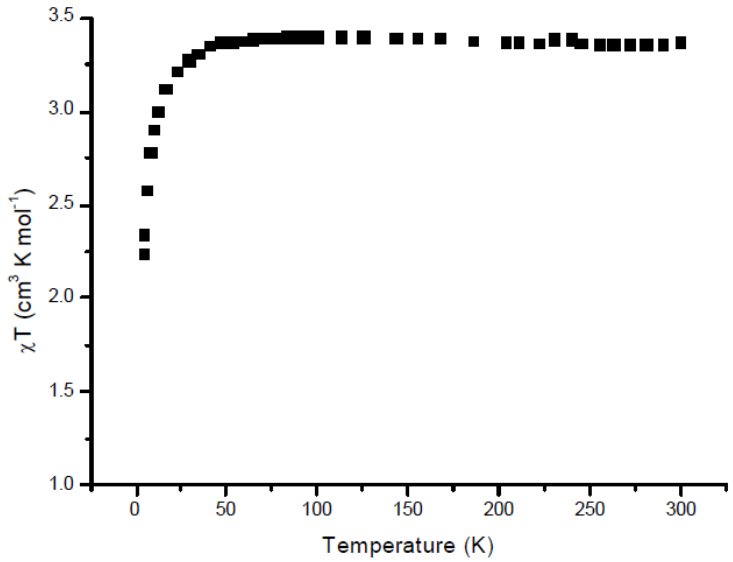

Figure S19. $\chi_M T$ versus temperature for **pin-S**.

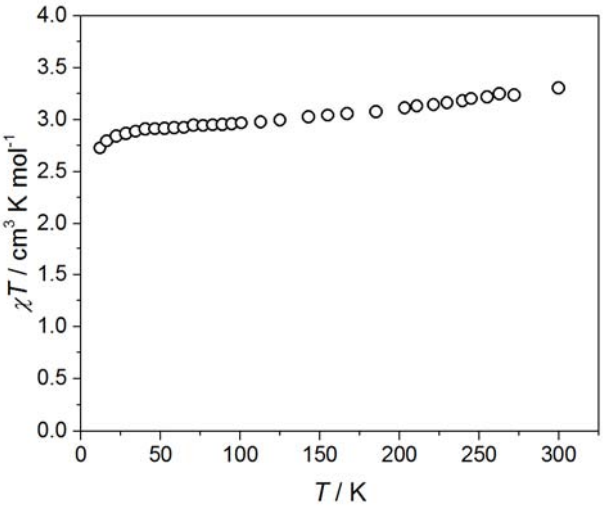

Figure S20. $\chi_M T$ versus temperature for **tvp-S**.

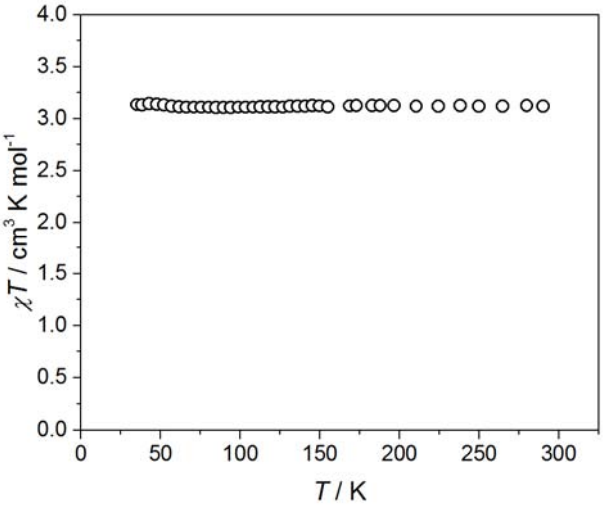

Figure S21. $\chi_M T$ versus temperature for **dbbpe-S**.

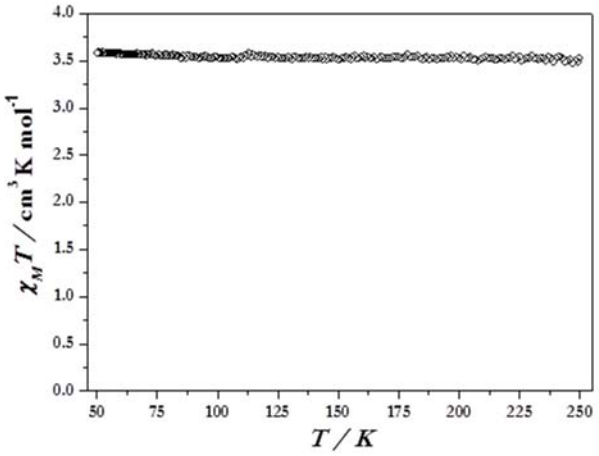

Figure S22. $\chi_M T$ versus temperature for **bptz-S**.

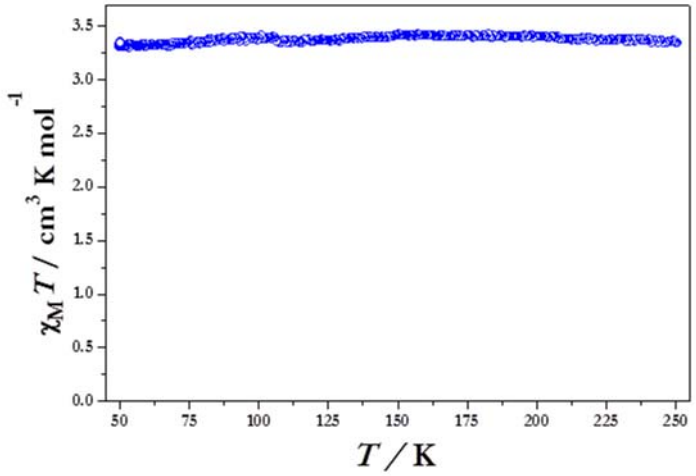

Figure S23. $\chi_M T$ versus temperature for **bptz-Se**.